JMEPEG (2007) 16:567–572
DOI: 10.1007/s11665-007-9068-5

1059-9495/$19.00

Slurry Erosion Studies on Surface Modified 13Cr-4Ni Steels: Effect of Angle of Impingement and Particle Size

T. Manisekaran, M. Kamaraj, S.M. Sharrif, and S.V. Joshi

(Submitted March 30, 2006; in revised form May 19, 2006)

Hydroturbine steels, such as 13Cr-4Ni martensitic steels, are generally subjected to heavy-erosive wear and loss of efficiency due to solid particulate entrainment in the water. Surface-modified steels have proven to give better performance in terms of erosive wear resistance. In the present study, an attempt is made to investigate the effect of angle of impingement and particle size on slurry-jet erosion behavior of pulsed plasma nitrided and laser hardened 13Cr-4Ni steels. Laser hardening process has shown good performance at all angles of impingement due to martensitic transformation of retained austenite. Plastic deformation mode of material removal was also an evident feature of all laser-hardened surface damage locations. However, pulsed-plasma nitrided steels have exhibited chip formation and micro-cutting mode of erosive wear. Erosion with 150-300 μm size was twice compared to 150 μm size slurry particulates.

Keywords angle of impingement, erosion damage, laser hardening, silt erosion, slurry-jet erosion, surface modification on 13Cr-Ni steels

1. Introduction

13Cr-4Ni steels are generally used for hydro turbines and water pumps. These are used because of their excellent mechanical properties and adequate corrosion resistance. However, these materials are considerably less resistant to erosive wear and get damaged due to excessive solid content entrained in the water. Erosive wear damage of components by silt results in drop in efficiency, forced outages and, repair. It has been reported that the silt erosion causes a loss of order of $120-150 million every year for hydro power stations (Ref 1, 2). To counteract the silt erosion problems, the surface of the components are suitably modified by hardening processes. In this regard, plasma nitriding and laser hardening find widespread use. It is well known that pulsed-plasma nitriding is widely preferred since this process offers some unique technical advantages (Ref 3, 4). In the present investigation, the effects of angle of impingement and particle size on the performance of surface modified 13Cr-4Ni steels by laser hardening and pulsed-plasma nitriding are reported. Scanning electron microscope observation of eroded pattern of steels at various impingement angles are presented and discussed.

T. Manisekaran and **M. Kamaraj**, Department of Metallurgical and Materials Engineering, Indian Institute of Technology, Madras, Chennai, Tamil Nadu 600 036, India; and **S.M. Sharrif** and **S.V. Joshi**, Centre for Laser Processing of Materials, International Advanced Research Centre for Powder Metallurgy and Newer Materials (ARCI), Hyderabad, AP 500005, India. Contact e-mail: kamaraj@iitm.ac.in.

2. Experimental

2.1 Materials and Surface Modifications

Cast 13Cr-4Ni (nominal composition of wt.0.058% C, 12.06% Cr, 3.85% Ni, 1.00% Mn 1.00% Si, 0.50% Mo and bal.Fe) martensitic stainless steel was used as the base material. These steels are generally used in quenched and tempered condition and, have a hardness of 310-315 HV. Samples of dimension of 50×50 mm^2 were machined from 6 mm thick cast 13Cr-4Ni steel plates. Laser hardening was carried out at ARCI Hyderabad using MIL-9 kW CO_2 laser system. Prior to the application of laser beam, the samples were coated with graphite. A laser beam of power of 3.2 kW with traversing speed of 40 mm/s was selected. The width of the laser beam used for hardening was kept 10 mm. Pulsed-plasma nitriding was carried out with following parameters.

Temperature: 500 °C
Time: 10 h
Current density: 1.3 mA/cm^2
Voltage: 1000 V
Pulse on-off time: 100 μs
Chamber atmosphere: 70% N_2-30% H_2

2.2 Characterization of Modified Steels

The microstructural details were studied using optical microscope. The hardness distribution across the cross section of modified steels was measured with Vickers micro-hardness tester with a load of 500 g. Scanning electron microscope was used to study the morphology of modified steels and identify the removal pattern in eroded steels.

2.3 Slurry Erosion Tests

A slurry-erosive wear test rig was used to study the slurry-erosive wear. The test facility consists of conical vessel of 10 L capacity, in which the slurry is mixed to the required

concentration. The samples are kept in holders and, it has a provision to vary the angle of the sample with respect to the jet. Slurry is pumped through the impeller system and directed towards the sample through the nozzle. The details of the test facility are given elsewhere (Ref 5). The tests were carried out as per ASTM G 73-98. A precision balance to an accuracy level of 0.01 mg was used to measure the mass loss occurring after certain test duration. Tests were carried to study the erosion performance of modified layers with two different erodent particle size ranges (less than 150 and 150-300 μm) for 2 h at 90°. The results have been plotted as cumulative erosion-time of exposure curves on co-ordinate of cumulative mass loss vs. time. The experimental test conditions are listed as below. The effect of angle of impingement was also studied at 30°, 45°, 60° and 90° for 1 h.

2.4 Experimental Test Conditions

Type of slurry: Silica and mixed in water
Hardness of the erodent: 110VHN
Test duration: 150 min
Concentration of the slurry: 10 kg/m^3
Size of the specimen: 50×50 mm^2
Jet distance: 100 mm
Nozzle dia.: 6 mm
Velocity of the slurry flow: 12 m/s

3. Results and Discussion

3.1 Characterization Details

Figure 1(a) shows the microstructure of the as-received material. It is mainly of needle shape martensite. Figure 1(b) shows the microstructure of the pulsed-plasma nitrided steels. It shows the presence of uniform white compound layer of thickness of 5 μm and the diffused zone below it. The layer formation was due to various nitrides formation, namely γ′-Fe_4N and ε-$Fe_{2-3}N$. Figure1(c) shows the microstructure of the laser-hardened steels. It shows the presence of white melted and resolidified layer and hardened zone below it. Retained austenite was embedded as granular morphology in martensite matrix. The total case depth comprising both melted white layer and hardened zone was around 160 μm. The martensite needles were refined in laser-hardened steels due to the high-cooling rates. The hardness distribution along the cross section of the laser-hardened steels is shown in Fig. 2(a). The hardness was higher in melted region in laser-hardened steels because of the formation of martensite due to very high cooling rates. However, this layer was not so hard since considerable amount retained austenite was also present in the melted zone. Figure 2(b) shows the hardness distribution across the cross section of pulsed-plasma nitrided steels. The main characteristic of hardness profile was a sharp decrease in hardness. The surface hardness obtained with pulsed-plasma nitrided steels was around 1500 HV. It is reported that the plasma nitriding of 13Cr-4Ni steels with continuous technique increased the hardness to merely 700 HV (Ref 3). This increase in hardness, in pulsed-plasma nitrided steels, may be due to the retention of more active nitrogen species for longer duration. XRD analysis

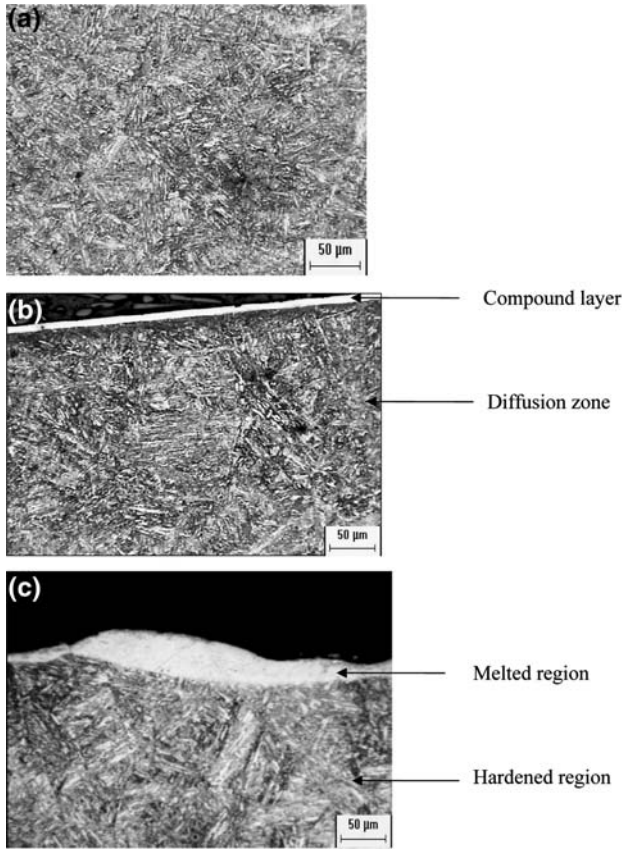

Fig. 1 Microstructure of (a) as received material (b) pulsed-plasma nitrided (c) Laser hardened

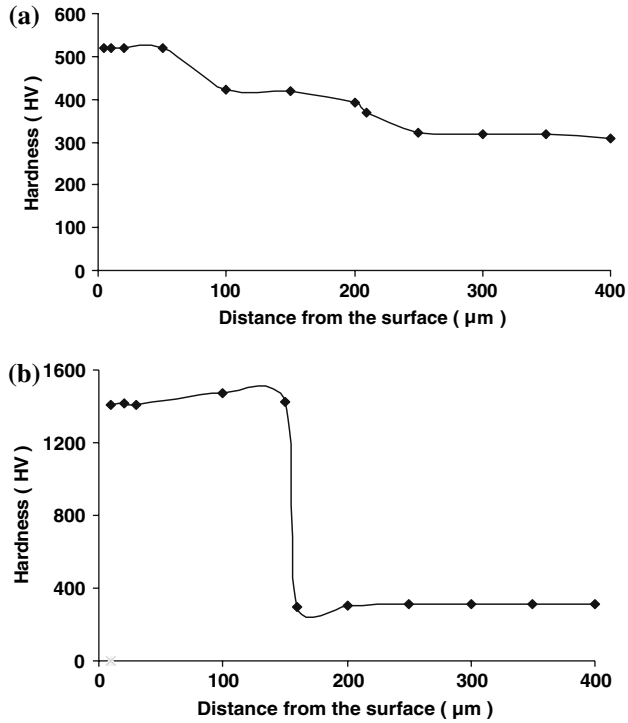

Fig. 2 Cross-sectional hardness distribution of (a) laser-hardened 13Cr-4Ni steels (b) pulsed-plasma nitrided 13Cr-4Ni steels

of laser-hardened 13Cr-4Ni steels confirmed the presence of retained austenite and precipitation of carbides. It is very common that laser-hardened steels contain certain amount of retained austenite (Ref 6, 7). The x-ray diffractogram study shows the presence of γ′ and ε iron nitrides and chromium nitride in pulsed-plasma nitrided 13Cr-4Ni steels. The results are shown in Fig. 3(a) and (b). Figure 4(a) shows the SEM micrograph of laser-hardened 13Cr-4Ni steels. The top layer corresponds to melted zone in which the carbide is dissolved as fine network. Below the melted zone the hardened region can be observed. The total treated layers were completely free from pores. Figure 4(b) shows the SEM micrograph of pulsed-plasma nitrided 13Cr-4Ni steels. The top gray band corresponds to the nitrided layer. Precipitation of CrN is observed in nitrided region. In the nitrided region, pores can be observed.

3.2 Erosion test Results

3.2.1 Effect of Angle of Impingement. Erosion of a material is dependent upon the angle at which the erodent particles strike the surface of the target (Ref 8-11). It has been found that maximum erosion rate for a ductile material is at impingement angle of approximately 20–30° and, it decreases at higher angles. This contrasts with brittle materials where the loss of material due to erosion rises steadily with angle, reaching a peak at 90° (Ref 11). Hence, coatings, which show good performance, close to or at near normal incidence angles may not exhibit the same performance at low-incidence angles. Thus, the effect of angle of impingement becomes an important parameter, since the silt entrained in water impinges at various incidence angles over the surface of the components in actual turbine atmosphere. Figure 5 shows the amount of erosion in terms of mass loss after 1 h of testing at various angles of impingement. It can be observed that the laser-hardened 13Cr-4Ni steel exhibited better performance than the pulse plasma nitrided 13Cr-4Ni steels especially, at low angles of impingement, for instance, at 30°. This is quite interesting, because the laser-hardened layer was not so hard as the pulsed-plasma nitrided layer, yet it had shown excellent performance at low angles of impingement. This might be due to the martensitic transformability of retained austenite upon repetitive plastic deformation at low angles of impingement. This transformation could have strengthened the laser-hardened layer against the erosion attack. Similar observations where the martensitic transformability played a role rather than increase in hardness was reported for the laser surface melted UNS S 42000 grade

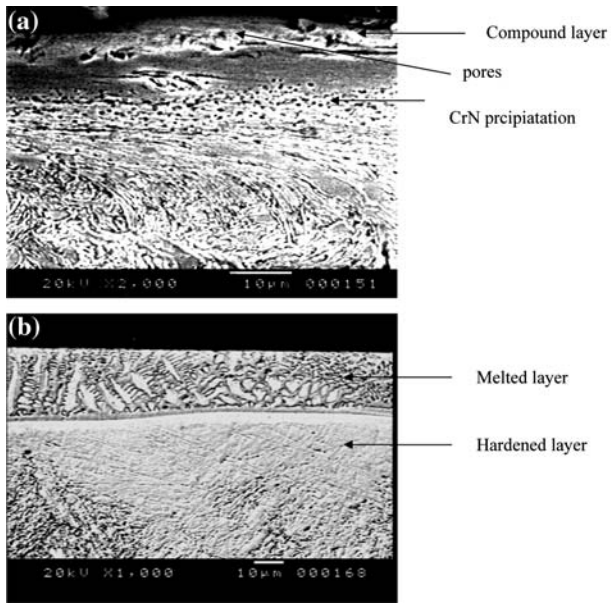

Fig. 4 SEM micrograph of (a) pulsed-plasma nitrided (b) laser-hardened steels

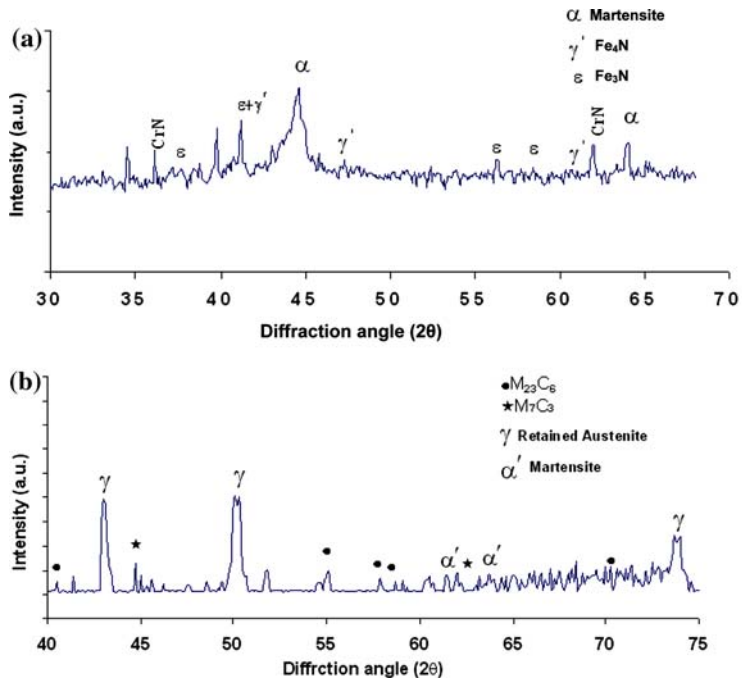

Fig. 3 X-ray diffractogram of (a) pulse plasma nitrided (b) laser-hardened steels

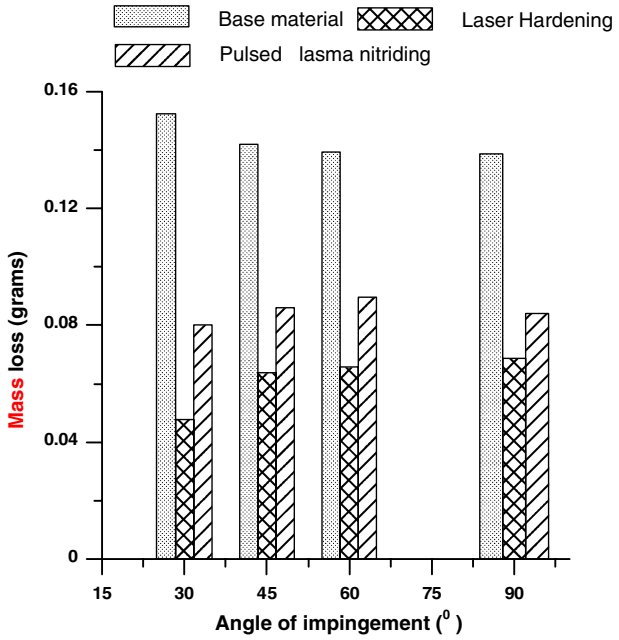

Fig. 5 Erosion loss for modified steels and as received material at various angles of impingement

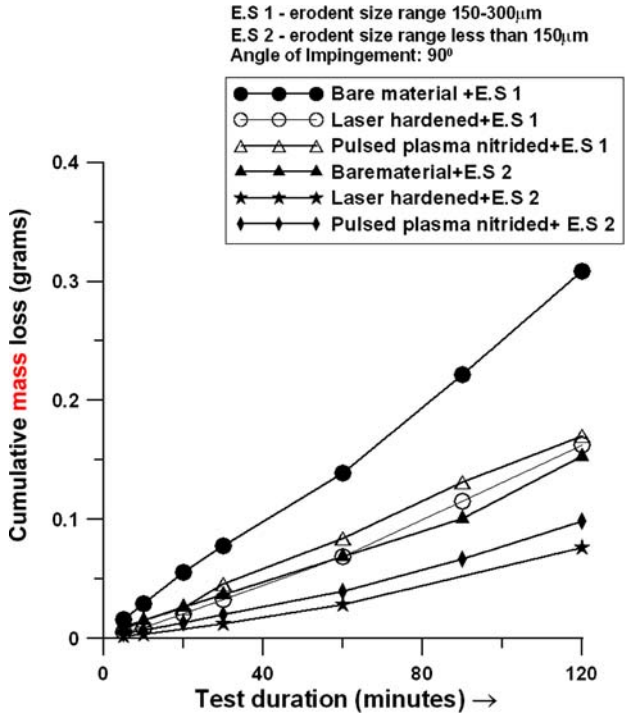

Fig. 6 Cumulative erosion curves for modified steels with two erodent size ranges

martensitic stainless steels in cavitation erosion (Ref 12). As much as threefold increase in erosion resistance for laser-hardened steels was observed at 30° compared to that of bare material at the same incidence angle. Pulsed-plasma nitrided steels enhanced erosion resistance only two times that of the bare material. This is because the nitrided layer was porous in nature and could not take up repetitive stresses as laser-hardened steels, in turn, resulting in the material removal by delamination (due to fatigue) and micro-cutting.

3.2.2 Effect of Particle Size. The particle size effect is generally taken as the change in erosion rate associated with changes in the size of erodent particles when nominally the same test conditions are used—test geometry, erodent mass, test velocity, and so on. The result of reducing the particle size in typical laboratory slurry erosion experiments is well known—the rate of erosion of the target decreases (Ref 13) However, there are number problems in conducting the tests with two different sized particles. This makes uncertainty in comparing the erosion rate with the use of two different sized erodent particles. With the change of particle size it is suggested that it may alter flow and impact conditions in laboratory simulated erosion testing and, thus significantly the erosion rate (Ref 14). In this investigation, the effect of erodent size range on erosion performance of surface modified 13Cr-4Ni steels is reported. Figure 6 shows the amount of erosion loss for bare material, and the modified steels for different size ranges. The trend in cumulative erosion curves was similar—there was no indication of any abrupt change in trend for the results of tests conducted with two different particle size ranges. Figure 7 shows as bar chart the amount of erosion after 2 h of testing at 90° incidence angles for modified steels and the bare material for different erodent size. It can be seen that amount of erosion loss with erodent particle size range 150-300 μm was two times more than the amount of erosion with erodent size range less than 150 μm. This reduced erosion may be due to the less impact energy apportioned to target surface by the fine erodent particles.

3.3 SEM of Eroded Steels

The mechanism of material removal in erosion largely depends on material properties and the angle at which the erodent strikes the surface of the target. Generally there are two mechanisms considered to be associated with the removal of material. They are repetitive plastic deformation and cutting. Ductile materials undergo mass loss by a process of direct microcutting or plastic deformation, followed by cutting. In brittle materials, the energy transfer associated with repeated particle impacts results in a fatigue process. Lateral and radial cracks, both surface and sub-surface, are formed and material is assumed to have been removed by the intersection of these cracks with each other, as well as with the surface (Ref 11). The mechanisms of material removal are considered to be different at low- and high-impact angles. When particles impact at surface at low angles of incidence, chip formation or cutting plays a role in material removal. Low-angle erosion may perhaps be compared to abrasion. Erosion at or close to normal incidence involves the formation of crater 'lips' of highly deformed material, which are subsequently removed as platelets after impact by a number of successive particles (Ref 14). Figure 8(a) shows the SEM micrograph of eroded surface of the as-received 13Cr-4Ni steels at 90° impingement after 1 h of testing. It can be observed that the material removal was due to extensive repetitive plastic deformation. The material was removed as platelets from highly deformed crater lips by successive impacts. Figure 8(b) shows the erosion pattern at 45 impingement angle. It can be visualized that the erosion pattern is similar to low angle abrasion. Figure 8(c) corresponds to SEM micrograph of the eroded pattern of as-received steels at 60°. It can be seen the removal was more in this case compared to 90° impingement. Figure 9(a) shows the SEM micrograph of eroded pattern of pulsed-plasma nitrided steels at

90 impingement angle. It can be observed that the material removal was due to plastic deformation followed by cutting. The lip formation was evident and the material was removed through the lip formation. Figure 9(b) shows the SEM micrograph of eroded pattern of pulsed-plasma nitrided steels at 90° impingement angle. It can be observed that the material removal was due to extensive microcutting through chip formation rather than by repetitive plastic deformation. Figure 10 shows the SEM micrograph of eroded surface of laser-hardened 13Cr-4Ni steels. It is evident from the pattern that material removal was due to repetitive plastic deformation.

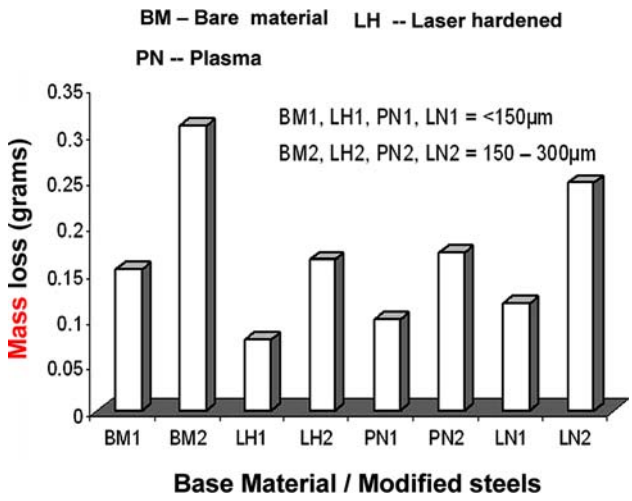

Fig. 7 Erosion loss for modified steels with different erodent sizes after 2 h

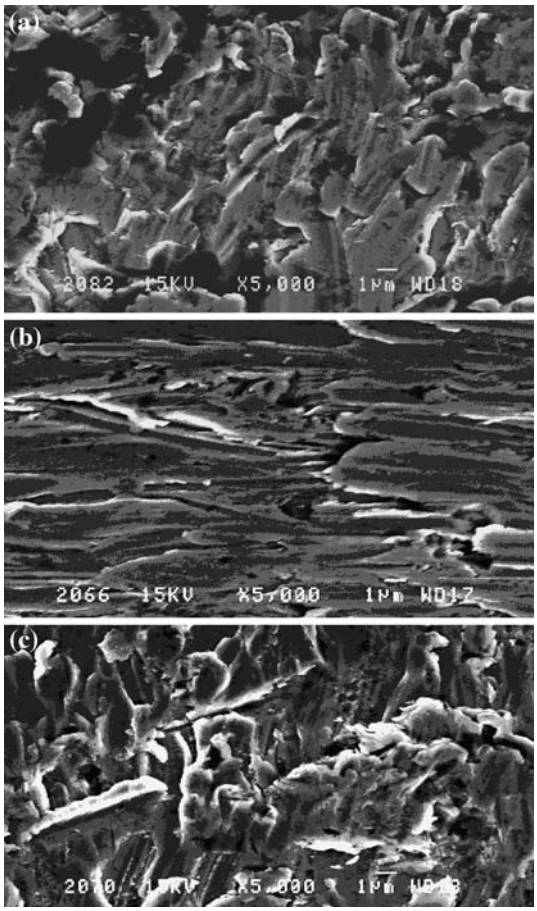

Fig. 8 SEM micrograph of eroded surface of as received 13Cr-4Ni steels at (a) 90° (b) 45° (c) 60° impingement angle

4. Conclusion

1. Laser hardening of 13Cr-4Ni steels exhibited better erosion resistance at all angles of impingement than pulse

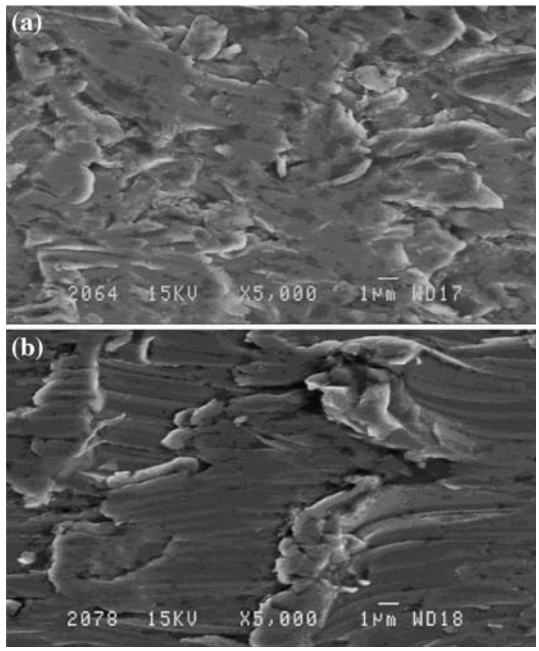

Fig. 9 SEM micrograph of eroded surface of pulsed-plasma nitrided 13Cr-4Ni steels at (a) 90° (b) 45° impingement

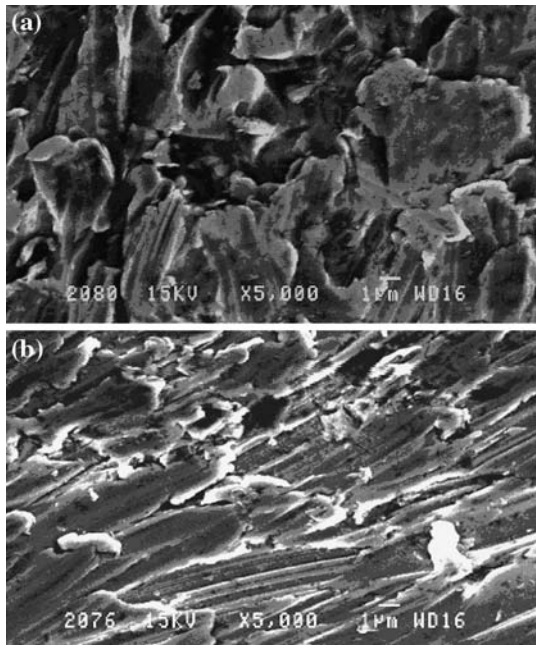

Fig. 10 SEM micrograph of eroded surface of laser-hardened 13Cr-4Ni steels at (a) 90° (b) 45° impingement

plasma nitriding. This may be attributed to martensitic transformability of the retained austenite coupled with moderate hardness. Pulsed-plasma nitrided steels could not withstand repetitive stresses arising out of jet impingement and, underwent chip formation and micro-cutting.

2. The amount of erosion with erodent size range 150-300 μm was two times more than the amount of erosion with erodent size range less than 150 μm.
3. SEM examination clearly revealed that plastic-deformation mode was primarily responsible for material removal in laser-hardened steels.

Acknowledgments

We wish to thank Dr. B.S. Mann, Additional director, Surface Coatings and Treatment Laboratory, Corporate R&D Division, BHEL, Vikasnagar, Hyderabad, India for his help in providing the material for this investigation. We also thank ARCI, Hyderabad for their assistance in Laser treatment of our Cr-Ni alloys. The authors are grateful to Department of Science and Technology (DST), India for their financial assistance.

References

1. B.S. Mann, Erosion Visualization and Characteristics of Two Dimensional Diffusion Treated Martensitic Stainless Steel Hydrofoils, *Wear*, 1998, **217**, p 56–61
2. B.S. Mann and V. Arya, Abrasive and Erosive Wear Characteristics of Plasma Nitriding and HVOF Coatings: Their Application in Hydro Turbines, *Wear*, 2001, **249**, p 354–360
3. B.S. Mann and V. Arya, An Experimental Study to Correlate Water Jet Impingement Erosion Resistance and Properties of Metallic Materials and Coatings, *Wear*, 2002, **253**, p 650–661
4. Y.M. Kim, J.U. Kim, and J.G. Han, Investigation on the Pulsed DC Plasma Nitriding with Optical Emission Spectroscopy, *Surf. Coat. Technol.*, 2002, **151-152** , p 227–232
5. R.J.K. Wood, The Sand Erosion Performance of Coatings, *Mater. Design*, 1999, **20**, p 179–191
6. K.H. Loa, F.T. Chenga, C.T. Kwok, and H.C. Man, Effects of Laser Treatments on Cavitation Erosion and Corrosion of AISI 440C Martensitic Stainless Steel, *Mater. Lett.*, 2003, **58**, p 88–93
7. C.T. Kwok, K.H. Lo, F.T. Cheng, and H.C. Man, Effect of Processing Conditions on the Corrosion Performance of Laser Surface-Melted AISI 440C Martensitic Stainless Steel, *Surf. Coat. Technol.*, 2003, **166**, p 221–230
8. Y.I. Oka, K. Okamura, and T. Yoshida, Practical Estimation of Erosion Damage Caused by Solid Particle Impact Part 1: Effects of Impact Parameters on a Predictive Equation, *Wear*, 2005, **259**(1–6), p 95–101
9. H.M. Clark and K.K. Wong, Impact Angle, Particle Energy and Mass Loss in Erosion by Dilute Slurries, *Wear*, 1995, **186-187**, p 454–464
10. G.W. Stachowiak, Particle Angularity and its Relationship to Abrasive and Erosive Wear, *Wear*, 2000, **241**, p 214–219
11. D.W. Wheeler and R.J.K. Wood, Erosion of Hard Surface Coatings for Use in Offshore Gate Valves, *Wear*, 2005, **258**, p 526–536
12. C.T. Kwok, H.C. Man, and F.T. Cheng, Cavitation Erosion and Pitting Corrosion Behaviour of Laser Surface-Melted Martensitic Stainless Steel UNS S42000, *Surf. Coat. Technol.*, 2000, **126**, p 238–255
13. H.M. Clark and R.B. Hartwich, A Re-Examination of the 'Particle Size Effect' in Slurry Erosion, *Wear*, 2001, **248**, p 147–161
14. D.J. O'Flynn, M.S. Bingley, M.S.A. Bradley, and A.J. Burnett, A Model to Predict the Solid Particle Erosion Rate of Metals and its Assessment Using Heat-Treated Steels, *Wear*, 2001, **248**, p 162–177